Enzymes Harboring Unnatural Amino Acids: Mechanistic and Structural Analysis of the Enhanced Catalytic Activity of a Glutathione Transferase Containing 5-Fluorotryptophan[†,‡]

James F. Parsons,[§] Gaoyi Xiao,[||] Gary L. Gilliland,[||] and Richard N. Armstrong*[,§]

Departments of Biochemistry and Chemistry and Center in Molecular Toxicology, Vanderbilt University School of Medicine, Nashville, Tennessee 37232-0146, and Center for Advanced Research in Biotechnology of the Maryland Biotechnology Institute, University of Maryland, Shady Grove, and of the National Institute of Standards and Technology, 9600 Gudelsky Drive, Rockville, Maryland 20850

Received January 28, 1998; Revised Manuscript Received March 3, 1998

ABSTRACT: The catalytic characteristics and structure of the M1-1 isoenzyme of rat glutathione (GSH) transferase in which all four tryptophan residues in each monomer are replaced with 5-fluorotryptophan are described. The fluorine-for-hydrogen substitution does not change the interaction of the enzyme with GSH even though two tryptophan residues (Trp7 and Trp45) are involved in direct hydrogen-bonding interactions with the substrate. The rate constants for association and dissociation of the peptide, measured by stopped-flow spectrometry, remain unchanged by the unnatural amino acid. The 5-FTrp-substituted enzyme exhibits a k_{cat} of 73 s^{-1} as compared to 18 s^{-1} for the native enzyme toward 1-chloro-2,4-dinitrobenzene. That the increase in the turnover number is due to an enhanced rate of product release in the mutant is confirmed by the kinetics of the approach to equilibrium for binding of the product. The crystal structure of the 5-FTrp-containing enzyme was solved at a resolution of 2.0 Å by difference Fourier techniques. The structure reveals local conformational changes in the structural elements that define the approach to the active site which are attributed to steric interactions of the fluorine atoms associated with 5-FTrp146 and 5-FTrp214 in domain II. These changes appear to result in the enhanced rate of product release. This structure represents the first of a protein substituted with 5-fluorotryptophan.

The global incorporation of unnatural amino acids in a protein at a selected set of codons can be accomplished in a few specific instances by expression of the protein in the presence of the unnatural amino acid. Although limited to unnatural amino acids that closely resemble the natural counterpart, the technique has been used widely and for some time for the incorporation of fluorinated aromatic amino acids in proteins as NMR probes of microenvironments (*1*−*10*). More recently, the technique has been used for the incorporation of selenomethionine as an isomorphous heavy atom derivative and strong anomalous scatterer for the solution of protein crystal structures by multiple isomorphous replacement and multiwavelength anomalous dispersion techniques (*11*). Despite decades of use as NMR probes, there is surprisingly little information on the structural and functional consequences of substitution of fluorine for hydrogen (e.g., as in 3-fluorotyrosine and 5- or 6-fluorotryptophan) in a protein context. Such substitutions are generally, and perhaps incorrectly, considered to be structurally benign.

Tryptophan residues are typically found imbedded in the interior of protein structures where the indole NH often acts as a hydrogen-bond donor. The fluorine-for-hydrogen substitution in 5-fluorotryptophan alters both the electronic and steric properties of the side chain. For example, the pK_a of the NH group of indole is reduced from 17 to 16.3 in 5-fluoroindole (*12*). A similar decrease is anticipated for the indole NH of 5-fluorotryptophan, making it a better hydrogen-bond donor. In addition, the van der Waals radius of fluorine is slightly larger than that of hydrogen. In fact, an aromatic C−F bond is 30% longer than the corresponding C−H bond. The extent to which these changes in the properties of the side chains affect protein structure and function have not been evaluated experimentally.

The glutathione transferases are a group of enzymes that catalyze the addition of the tripeptide glutathione (GSH)[1] to a wide variety of electrophilic compounds (*13*). The enzymes are very well characterized, both structurally and mechanistically, and thus provide an excellent vehicle for evaluation of both the structural and mechanistic consequences of substitutions of unnatural amino acids. For example, in the case of the M1-1 glutathione transferase from rat, the active site contains two tryptophan residues, Trp7 and Trp45, each of which acts as a hydrogen-bond donor to enzyme-bound GSH (Figure 1). In addition, it is well established that a hydrogen bond between the hydroxyl group of Tyr6 and the sulfur of the peptide stabilizes the thiolate

[†] Supported by Grants R01 GM30910 and P30 ES00267 from the National Institutes of Health.

[‡] The final coordinates for the structure have been deposited with the Brookhaven Protein Data Bank under the file name 5FWG.

* Address correspondence to this author.

[§] Vanderbilt University.

[||] Center for Advanced Research in Biotechnology.

[1] Abbreviations: GSH, glutathione; GSO_3^-, glutathione sulfonate; CDNB, 1-chloro-2,4-dinitrobenzene; GSDNP, *S*-(2,4-dinitrophenyl)-glutathione; 5-FTrp, 5-fluorotryptophan; CAPS, 3-(cyclohexylamino)-1-propanesulfonic acid.

S0006-2960(98)00219-0 CCC: $15.00
Published on Web 04/14/1998

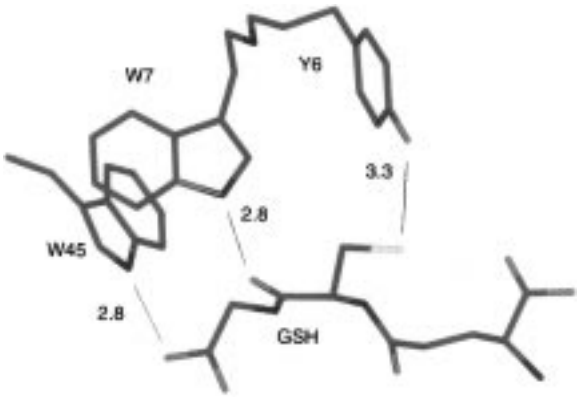

FIGURE 1: Hydrogen-bonding interactions between GSH and tyrosine and tryptophan residues in the active site of the M1-1 glutathione transferase in complex with (*9R,10R*)-9-(*S*-glutathionyl)-10-hydroxy-9,10-dihydrophenanthrene taken from PDB coordinate file 3GST. Only the glutathionyl portion of the product inhibitor is shown for clarity. The hydrogen-bond distances between Trp7 and the carbonyl oxygen, Trp45 and the carboxyl oxygen, and Tyr6 and the sulfur of GSH are given in angstroms.

nucleophile (*14*, *15*). We have previously shown that the quantitative incorporation of 3-fluorotyrosine can be a useful tool for assessing the role of the tyrosyl hydroxyl group in catalysis (*16*). To gain further insight into the role of the Trp residues in catalysis and to extend our studies with unnatural amino acids, we have produced an enzyme in which all four tryptophan residues are replaced by the unnatural amino acid 5-fluorotryptophan.

Here we describe the near-quantitative incorporation of 5-fluorotryptophan into the rat M1-1 glutathione transferase, the altered catalytic characteristics of the enzyme, and finally the three-dimensional structure of the protein as determined by X-ray crystallography. This structure represents the first of a protein substituted with 5-fluorotryptophan and complements the structure of the tetradeca(3-fluorotyrosyl)-glutathione transferase (*17*). Together the structures provide a library of microenvironments from which the effects of fluorine substitution in proteins can be evaluated. In addition, the results delineate the utility and limitations of unnatural amino acids as mechanistic and structural probes of enzymes.

EXPERIMENTAL PROCEDURES[2]

Expression and Purification of Tetra(5-fluorotryptophanyl)glutathione Transferase. The rat M1-1 glutathione transferase with all four tryptophan residues replaced by the unnatural amino acid 5-fluorotryptophan was expressed in *Escherichia coli* essentially as previously described for the 3-fluorotyrosine substituted M1-1 enzyme (*16*, *17*). Briefly, *E. coli* strain BL21(DE3) transformed with the expression plasmid was grown to log phase in 1 L of minimal medium supplemented with 0.2 mM of each amino acid except tryptophan, 0.4% glucose, 50 mg/L thiamine, 50 mg/L uracil, and 20 mg/L biotin. Two grams of racemic 5-fluorotryptophan was added to the culture 10 min prior to induction of transcription by IPTG. For crystallization, the enzyme was purified by affinity chromatography on a GSH−agarose column equilibrated with 10 mM Tris and 1 mM EDTA (pH 7.8). After application of the cell extract, the column was washed with >50 column volumes of the same buffer containing 0.2 M KCl. The enzyme was eluted with 20 mM Tris, 1 mM EDTA, 0.2 M KCl, and 1 mM DTT, containing 50 mM GSH (pH 7.0). When completely ligand-free enzyme was needed for stopped-flow experiments, the enzyme was purified on an *S*-hexyl−GSH Sepharose column. In this case the enzyme was eluted with 50 mM CAPS containing 1 mM EDTA, 1 mM DTT, and 1.0 M KCl (pH 9.8). The pH of the collected fractions was immediately changed back to 7.0. In all cases, fractions containing GSH transferase activity were pooled, concentrated and dialyzed against 10 mM KH_2PO_4, 1 mM EDTA, and 1 mM DTT (pH 7.0).

Analysis of 5-Fluorotryptophan Incorporation. Two milligrams of enzyme was hydrolyzed under vacuum in 4 M KOH at 120 °C for 18 h. The residue was then analyzed by HPLC as follows. The hydrolysis mixture was evaporated to dryness and redissolved in 100 μL of mobile phase composed of 20% methanol in 0.2 M ammonium acetate, pH 3.8. Ten microliters of the mixture was injected onto a Beckman Ultrasphere C18 column (4.6 × 250 mm) which was eluted isocratically at a flow rate of 1.0 mL/min with detection at 280 nm. Tryptophan eluted at approximately 9 min and 5-fluorotryptophan at approximately 12 min. The relative amount of each in the protein was determined from the areas of the corresponding peaks. The areas were corrected for the small difference in extinction coefficient between the two compounds at 280 nm. Electrospray ionization mass spectra of the fluorinated and native enzymes were obtained on a Finnigan TSQ 7000 mass spectrometer using a carrier solvent of 50% methanol and 0.5% acetic acid.

Steady-State Kinetics. The steady-state kinetics of the enzyme-catalyzed addition of GSH to 1-chloro-2,4-dinitrobenzene (CDNB) and the spectroscopic pK_a of enzyme-bound GSH were measured as previously described (*15*). The pH dependence of the reaction with CDNB was measured as described by Liu et al. (*15*). The programs Grafit (*18*) and HABELL (*19*) were used to extract kinetic constants from the data. The turnover numbers of the enzymes toward phenanthrene 9,10-oxide and 4-phenyl-3-buten-2-one were estimated from reactions run with saturating concentrations of each substrate at pH 7.0 and 6.5, respectively (*20*).

Determination of Rate Constants by Stopped-Flow Spectrophotometry. The rate constants for binding and release of GSH from the native and tetra(5-fluorotryptophanyl)-glutathione transferase were determined using an Applied Photophysics SX-17MV stopped-flow spectrometer. Binding of glutathione was monitored by the increase in optical density at 239 nm. One syringe contained 5 μM ligand-free enzyme in 100 mM KH_2PO_4 (pH 7.0) while the other syringe contained a variable concentration of GSH in the same buffer. Upon mixing, a burst corresponding to the ionization of GSH on the enzyme surface is seen at 239 nm ($\Delta\epsilon$ = 5000 M^{-1} cm^{-1}). The binding of glutathione sulfonate (GSO_3^-) and the product, 2,4-dinitrophenylglutathione (GSDNP), were monitored with the same instrumentation operated in the fluorescence mode with excitation of the protein at 290 nm and observation of the total intrinsic protein fluorescence through a 320 nm cutoff filter.

[2] Certain commercial equipment, instruments, and materials are identified in this paper in order to specify the experimental procedure as completely as possible. In no case does such identification imply a recommendation or endorsement by the National Institute of Standards and Technology nor does it imply that the material, instrument, or equipment identified is the best available for the purpose.

Table 1: Data Collection and Refinement Statistics for $(5\text{-FTrp})_4$ Glutathione Transferase Complexed with (*9R,10R*)-9-(*S*-Glutathionyl)-10-hydroxy-9,10-dihydrophenanthrene

Data Collection	
D_{min} (Å)	2.0
space group	*C*2
asymmetric unit	1 dimer
unit cell parameters	$a = 88.6$ Å, $b = 68.7$ Å, $c = 80.7$ Å, $\alpha = 105.1°$
observations	184 888
unique reflections	29 587
completeness (%)	95 (68.3)[a]
average $I/\sigma(I)$	16.3 (9.1)[a]
R_{merge}[b]	0.066
Refinement	
resolution range (Å)	65.0−2.0
reflections used with $I \geq 2\sigma(I)$	28 444
crystallographic *R*-factor[c]	0.181
non-hydrogen protein atoms	3644
product atoms	70
water molecules	376
rms deviation from ideal	
bond distances (Å)	0.022
bond angles (deg)	3.03
planar groups (Å)	0.020

[a] Numbers in parentheses are for the last resolution shell (2.07−2.0 Å). [b] $R_{merge} = \sum|I - \langle I\rangle|/\sum I$. [c] $R_{cryst} = \sum_{hkl}||F_o| - |F_c||/\sum_{hkl}|F_0|$

Crystallization. Crystals of the $(5\text{-FTrp})_4$ enzyme were grown by the hanging-drop vapor-diffusion method at room temperature (22 °C). Each 7 μL drop initially contained 10 mg/mL protein, 2 mM product inhibitor (*9R,10R*)-9-(*S*-glutathionyl)-10-hydroxy-9,10-dihydrophenanthrene, 0.3% *n*-octyl β-D-glucopyranoside, 10% poly(ethylene glycol) 3000, and 100 mM HEPES buffer (pH 7.6). The drops were equilibrated against wells containing 1 mL of 24% PEG 3000. Crystals of the same habit as the native protein (space group *C*2) grew in 1−4 days.

X-ray Data Collection. A single crystal of approximate dimensions 0.2 × 0.2 × 0.5 mm was mounted on a nylon loop, flash-frozen, and maintained at −170 °C with stream of cold nitrogen during the entire data collection. X-ray diffraction data were collected using an Rigaku R-axis IIc image plate set 110 mm from the crystal. X-rays were generated by an Rigaku RU-200 rotating copper anode source operating at 5 kW (100 mA, 50 kV). The detector image scan width was 1.0° in ω. Exposures of 20 min/deg of oscillation range were used. One hundred eighty degrees of data were collected. The raw data were processed, scaled, and reduced using the HKL software package (*21*) on a Silicon Graphics Indigo2 workstation.

Structure Solution and Refinement. Crystals of tetra(5-fluorotryptophanyl)glutathione transferase were isomorphous with those of the native enzyme (Table 1). That structure (PDB file 3GST) was therefore used as a starting model for a direct replacement solution. All water molecules and the product molecules were deleted from the probe model. Simulated annealing and rigid-body refinement were carried out first using X-PLOR (*22*). The *R*-factor at this point was 0.47. Clear electron density was seen for the fluorine atoms on all eight 5-FTrp residues in the dimer. All further refinement was done using the program TNT (*23*) after construction of a refinement dictionary for 5-fluorotryptophan using a model built and minimized with the program package Quanta 4.1.1. The program O (*24*) was used between refinement cycles for map inspection and manual model building. The *R*-factor dropped steadily as the product and solvent molecules were added. PROCHECK (*25*) was used to assess the stereochemical quality of the model. The refinement statistics are summarized in Table 1.

Table 2: Steady-State Kinetic Constants for the Native and $(5\text{-FTrp})_4$ Enzyme

	enzyme	
	native	5-FTrp
k_{cat} (s^{-1})	18 ± 2	73 ± 3
K_m^{GSH} (μM)	36 ± 4	55 ± 3
k_{cat}/K_m^{CDNB} (M^{-1} s^{-1})[a]	$(1.0 \pm 0.1) \times 10^6$	$(2.1 \pm 0.2) \times 10^6$
K_m^{CDNB} (μM)	41 ± 4	55 ± 4
pK_a (kinetic)[b]	6.2 ± 0.3	6.5 ± 0.2
pK_a (spectroscopic)[c]	6.6 ± 0.2	6.9 ± 0.2
k_{cat}^{PO} (s^{-1})[d]	0.19 ± 0.02	0.21 ± 0.02
k_{cat}^{PBO} (s^{-1})[e]	0.11 ± 0.01	0.13 ± 0.01

[a] Limiting value of k_{cat}/K_m at high pH. [b] Determined from the pH dependence of k_{cat}/K_m^{CDNB}. [c] Determined by UV−visible difference spectroscopy as described previously (*15*). [d] Phenanthrene 9,10-oxide. [e] 4-Phenyl-3-buten-2-one.

RESULTS

Expression and Catalytic Properties of $(5\text{-FTrp})_4$ Glutathione Transferase. The $(5\text{-FTrp})_4$ enzyme was efficiently expressed in *E. coli* (ca. 50 mg/L of culture) in the presence of 5-fluorotryptophan. Amino acid analysis revealed that the enrichment in the unnatural amino acid was ≥95%. Electrospray ionization mass spectrometry indicated a molecular mass of 25 863 ± 3 Da for the fluorinated enzyme and 25 790 ± 3 Da for the native enzyme, a difference of 73 Da, which is in excellent agreement with the expected 72 Da mass difference. Interestingly, the incorporation of 5-FTrp results in an enzyme with slightly greater catalytic efficiency than the native enzyme toward 1-chloro-2,4-dinitrobenzene, a substrate for which product release is the rate-limiting step (*20*). Steady-state kinetic analysis of the mutant reveals that the turnover number, k_{cat}, is nearly 4 times higher than is observed with the native enzyme and that the limiting value of k_{cat}/K_m at high pH was increased greater than 2-fold (Table 2). In contrast, the turnover numbers for two substrates, phenanthrene 9,10-oxide and 4-phenyl-3-buten-2-one, for which the chemical step is known to be rate-limiting are unchanged by the incorporation of 5-FTrp. Finally, there is no detectable change in the apparent spectroscopic or kinetic pK_a of the sulfhydryl group of enzyme-bound GSH (Table 2).

Although two Trp residues interact directly with the substrate GSH, the $(5\text{-FTrp})_4$ enzyme exhibits no significant differences in the binding of the peptide or in the ionization of the sulfhydryl group. The preequilibrium binding of GSH to the native and mutant enzymes can be monitored by observing the increase in A_{239} due to ionization of the thiol on binding to the enzyme as shown in Figure 2A. Neither the apparent second-order rate constant for binding, obtained from the dependence of the observed rate constant on [GSH], nor the off rate for GSH from the mutant was significantly different than the rate constants for the native enzyme (Figure 2B and Table 3). The apparent dissociation constant for the native enzyme calculated from $K_d = k_{off}/k_{on} = 26$ μM is in reasonable agreement with the values (7−22 μM) obtained

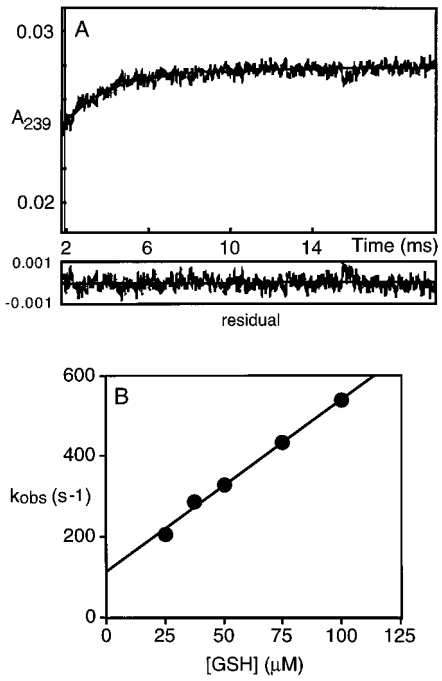

FIGURE 2: (A) Observed absorbance change at 239 nm on mixing 5 μM native enzyme and 75 μM GSH at pH 7 and 25 °C. The data are fit to a single exponential with $k_{obs} = 450 \pm 10$ s^{-1}. (B) Dependence of k_{obs} on the concentration of GSH. The solid line is a fit to the equation $k_{obs} = k_{on}[GSH] + k_{off}$ with $k_{on} = (4.3 \pm 0.2) \times 10^6$ M^{-1} s^{-1} and $k_{off} = 111 \pm 13$ s^{-1}.

Table 3: Rate Constants for Binding and Release of Ligands with the Native and $(5\text{-FTrp})_4$ Enzymes[a]

enzyme/ligand	k_{on} (M^{-1} s^{-1})	k_{off} (s^{-1})	K_d[b] (μM)
native/GSH	$(4.3 \pm 0.2) \times 10^6$	111 ± 13	26 ± 3
5-FTrp/GSH	$(4.9 \pm 0.1) \times 10^6$	99 ± 4	20 ± 1
5-FTrp/GSO_3^- [c]	$(2.4 \pm 0.1) \times 10^6$	<5	<2
native/GSDNP	$(3.2 \pm 0.2) \times 10^7$	28 ± 8	0.9 ± 0.3
5-FTrp/GSDNP	$(3.6 \pm 0.2) \times 10^7$	63 ± 7	1.8 ± 0.2

[a] All rate constants were determined from the concentration dependence of the relaxation kinetics for approach to equilibrium under pseudo-first-order conditions with ligand in excess as described in the Experimental Procedures. [b] Calculated from k_{off}/k_{on}. [c] A fluorescence signal for binding of GSO_3^- could not be observed for the native enzyme.

in equilibrium binding studies (*26, 27*). It is notable that the rate constant for binding of GSH to either enzyme is significantly less than the diffusion limit.

Interestingly, the incorporation of 5-FTrp into the enzyme alters the spectral properties of the protein such that there is a large increase in the intrinsic protein fluorescence on association of the tight-binding preionized analogue of GSH, glutathione sulfonate (GSO_3^-). The change is sufficient to permit monitoring of the binding of GSO_3^- in the stopped flow (data not shown). The k_{on} for GSO_3^- is nearly the same as that for GSH, while k_{off} is at least 20-fold smaller (Table 3).

There is a significant decrease in the intrinsic protein fluorescence of both the native and $(5\text{-FTrp})_4$ enzyme on binding the product *S*-(2,4-dinitrophenyl)glutathione (GSDNP), which can be exploited to monitor the binding equilibrium (data not shown). The kinetics of binding of the product is quite distinct in several respects from that observed for GSH (Table 3). First, k_{on} for the product is about 10-fold greater than that for GSH, so that it begins to approach the expected diffusion limit of 10^8 M^{-1} s^{-1}. Second, there is a distinct and easily measurable difference in k_{off} for the product with the native and $(5\text{-FTrp})_4$ enzymes. Third, the values of k_{off} correspond, within experimental error, to the turnover numbers of the two enzymes in the addition of GSH to CDNB. The latter fact indicates that the incorporation of the fluorine alters the kinetic properties of the enzyme primarily by enhancing the rate of product release. The possible structural basis for this observation is discussed below.

Crystal Structure of Tetra(5-fluorotryptophanyl)glutathione Transferase. The overall structure of the mutant enzyme is very similar to that of the native protein (Figure 3). The final model consisting of 434 residues, two product molecules, and 376 water molecules had good geometry with 89.4% of the residues falling within the most favorable region of the $\varphi-\psi$ plot according to the verification program PROCHECK. Only one residue, Ala212 in the B subunit, was listed as an outlier. Structural alignment of the 434 α-carbon atoms of the mutant and the native enzyme dimers yields an RMS deviation of 0.38 Å. Clear electron density was seen for all eight 5-FTrp residues in the asymmetric unit as exemplified in Figure 4. One part of the structure that did not show well-defined electron density was the phenanthrenyl portion of the product inhibitor (*9R,10R*)-9-(*S*-glutathionyl)-10-hydroxy-9,10-dihydrophenanthrene bound at the active site. This stands in contrast to the excellent electron density seen for all parts of the inhibitor bound to the native enzyme (*28*).

Structure of the GSH Binding Domain. The two Trp residues (Trp7 and Trp45) that participate as hydrogen-bond donors to the bound peptide (Figure 1) are located in the GSH binding domain (domain I) of the enzyme. Although residues near the active site of the $(5\text{-FTrp})_4$ GSH transferase exhibit some noteworthy differences compared to the native enzyme, the positions of the two active-site 5-FTrp residues are little changed (Figure 5) and the aforementioned hydrogen bonds in the product complex are maintained. The most notable difference in domain I is associated with the residue following 5-FTrp7, Asn8, which has its side chain pointing toward the surface of the enzyme. The residue is in a much different orientation compared to the native structure. The fluorine atom of 5-FTrp7 is in close van der Waals contact with the carbonyl oxygen of Ala33 (Figure 5B), an interaction that causes a displacement of the main chain at residue 8. Moreover, the side chain exhibits poor electron density beyond CB in both subunits. Why the movement of the main chain causes a loss of well-defined electron density for the side chain of Asn8 is unclear. In any event Asn8 is known not to participate in catalysis (*29*).

The interaction between the sulfur of GSH and the hydroxyl group of Tyr6, a crucial residue in catalysis, is not significantly perturbed in the $(5\text{-FTrp})_4$ enzyme. The oxygen remains 3.2 Å from the sulfur of the thioether product, consistent with its role as a hydrogen-bond donor to the sulfur. There are some small changes in the geometry of Thr13, a residue previously shown to modulate catalysis via an on-face hydrogen bond with the π system of Tyr6. In the native M1-1 structure, the γ-oxygen is about 3.4 Å distant from the centroid of the aromatic ring in each subunit. The interactions are somewhat different in the 5-FTrp mutant.

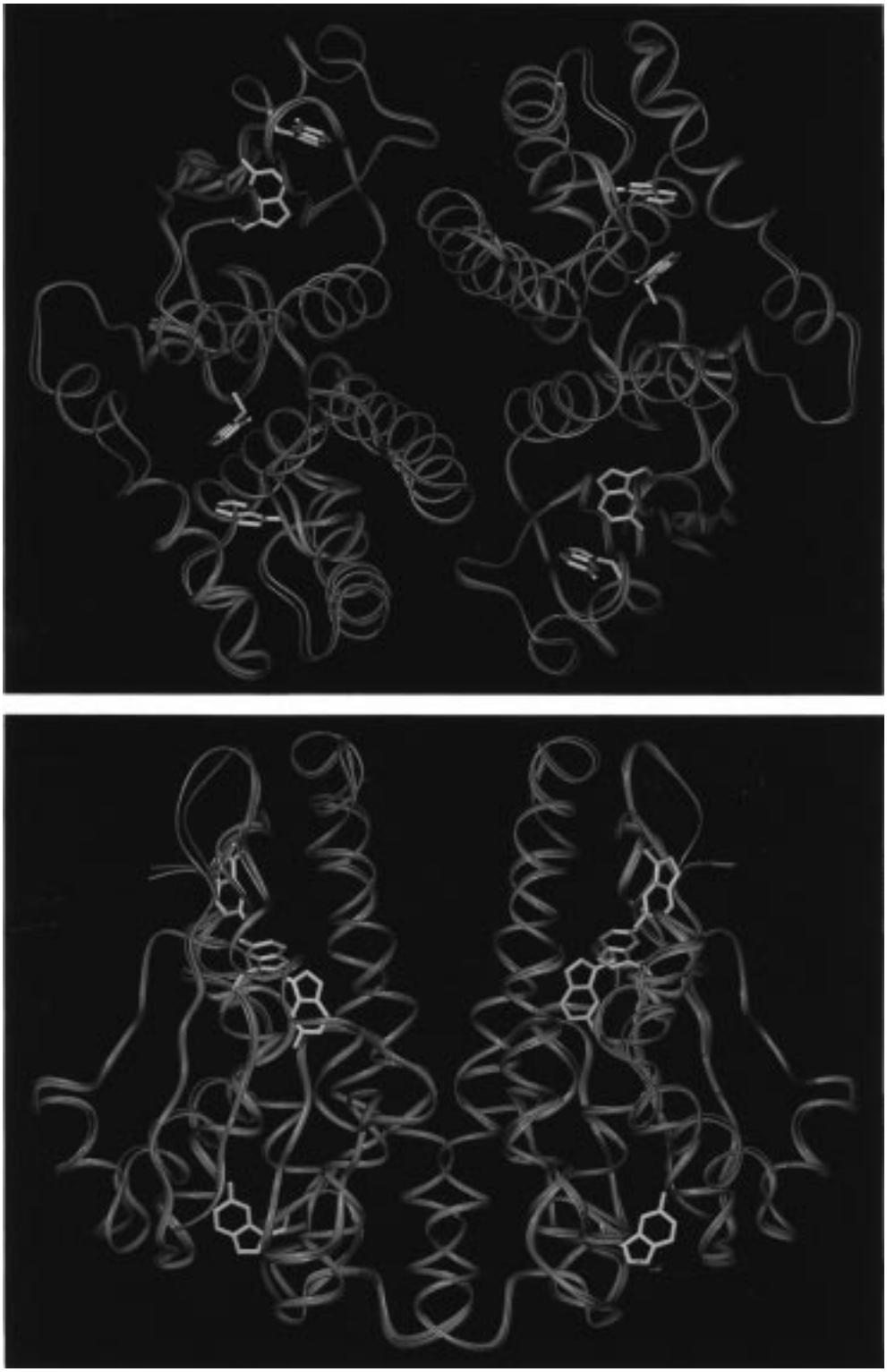

FIGURE 3: Ribbon trace of the $(5\text{-FTrp})_4$ enzyme viewed down (A, top) and perpendicular to (B, bottom) the noncrystallographic 2-fold axis relating the subunits in the dimer. The traces of the native and $(5\text{-FTrp})_4$ enzymes are shown in purple and green, respectively. The 5-FTrp residues are illustrated in yellow.

In one subunit, the γ-oxygen of Thr13 is directly above the plane of the aromatic ring of Tyr6 and is just 3.05 Å from the centroid of the ring. In the other subunit, the geometry of the side chain is altered such that the γ-carbon, not the γ-oxygen, is interacting with the aromatic ring. The density is quite convincing in each case. This change might be expected to affect catalysis since previous experiments with the mutants T13A, T13V, and T13S has shown that the loss of the on-face hydrogen bonding interaction leads to an increase in the pK_a of the enzyme-bound GSH by 0.7 pK units (*30, 31*). However, analysis of the pH dependence of the kinetics and spectral properties of the $(5\text{-FTrp})_4$ enzyme does not reveal any noteworthy change (Table 2).

Structure of Domain II. The two 5-fluorotryptophan residues in domain II, 5-FTrp146 and 5-FTrp214, seem to have a greater effect on the structure and the catalytic

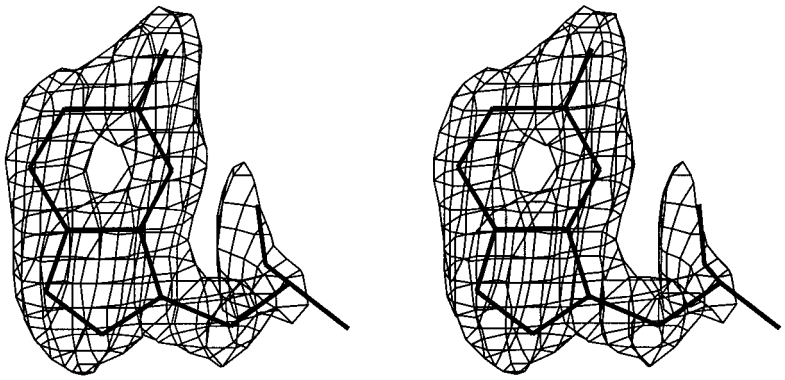

FIGURE 4: Stereoview of the final $2F_o - F_c$ electron density for 5-FTrp45 in subunit A contoured at 1.5 σ.

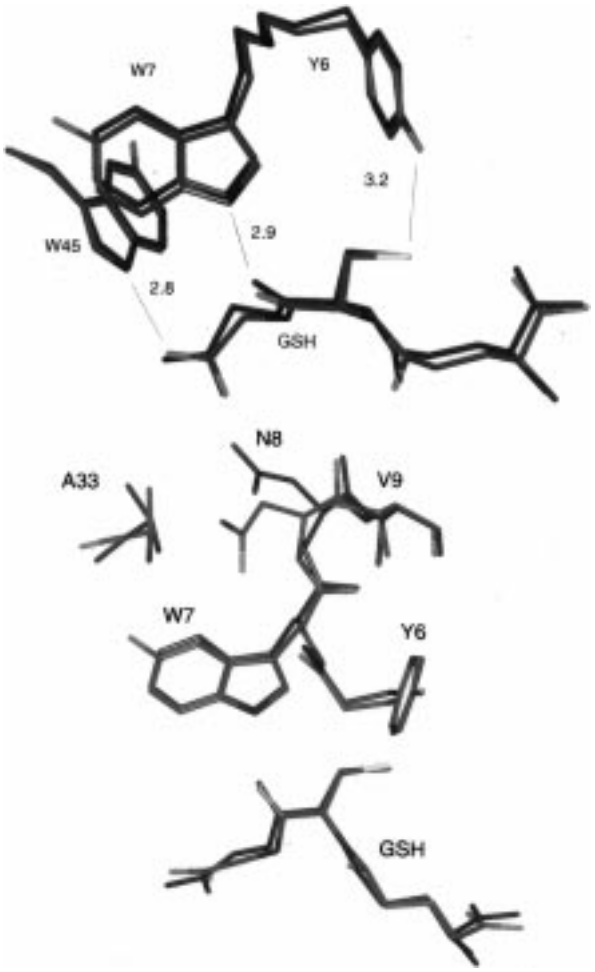

FIGURE 5: (A, top) Superposition of the selected active-site residues and GSH for the native (3GST, shown in blue) and mutant (5FWG) structures. Only the glutathionyl-portion of the product is shown for clarity. The hydrogen bonding distances in 5FWG (subunit B) are shown for comparison to those for the native enzyme illustrated in Figure 1. (B, bottom) Illustration of main-chain displacement near 5-FTrp7 due to the steric interaction between the fluorine atom of 5-FTrp7 and the carbonyl oxygen of Ala33.

behavior of the enzyme than do 5-FTrp7 and 5-FTrp45 located in domain I. This is suggested by three facts. First, in both subunits, there are significant RMS deviations in the positions of the CA atoms for these or associated residues (Table 4). Second, analysis of the temperature factors for atoms at the C-terminal end of the α4 helix (residues 104−115) reveals that the average *B*-factor for all side-chain atoms on the helix (41 Å^2) is 23% higher than the average *B*-factor

Table 4: Selected RMS Differences in CA Positions between the Structures of Tetra(5-fluorotryptophanyl)glutathione Transferase and the Native Enzyme[a]

	RMSD[b] (Å)	
residue	subunit A (0.33 Å)	subunit B (0.40 Å)
Tyr6	0.25	0.24
5-FTrp7	**0.44**	0.39
Asn8	**0.62**	**0.82**
Asn44	**0.46**	0.11
5-FTrp45	0.24	0.15
Tyr115	0.23	0.15
Pro145	**0.77**	**0.68**
5-FTrp146	**0.45**	0.16
Ser209	0.23	0.36
5-FTrp214	0.15	0.41
Ser215	0.24	**0.79**
Asn216	**0.53**	**0.57**

[a] Coordinates of the native enzyme are from PDB file 3GST (*28*). [b] The RMS differences are calculated by superposition of the individual subunits. Significant positive deviations from the average RMSD are shown in bold. For easy comparison, the average RMS deviation in the CA positions for each subunit is given in parentheses.

(33.4 Å^2) for all protein atoms in the structure. In contrast, there is only a 4% difference in the same average *B*-factors for the native structure (19.1 Å^2 for helix 4 vs 18.3 Å^2 for all atoms). Thus, the side chains associated with the portion of helix 4 that defines the product binding site appear to be either somewhat more mobile in the mutant or possess a greater degree of static disorder in the frozen crystal.[3] Finally, the poor electron density for the phenanthrenyl portion of the product suggests that the interactions between the xenobiotic substrate binding site and the product have been significantly disrupted. The possible structural basis for this is summarized below.

The structural deviations in the C-terminal tail appear to be due to unfavorable van der Waals contacts between the fluorine atom of 5-FTrp214 and CD1 of Ile207 and CE2 of Phe208. This effect is transmitted along the chain to the

[3] Although the trends in averaged *B*-factors support the notion that this portion of the active site in the 5-FTrp-substituted enzyme exhibits higher mobility or a greater degree of static disorder, the comparison with the native enzyme must be viewed with some caution. Different strategies were used in the refinement of the two models. The final refinement of the native (3GST) structure was accomplished with PROLSQ, while 5FWG was refined using the TNT program package. In our experience TNT generally gives higher *B*-factors as reflected in the averaged *B*-factors for the two. Given the considerable difference in the average *B*-factors for the two structures and the differences in the way *B*-factors are treated in refinement strategies used, it is not clear that even normalized trends in *B*-factors are meaningful.

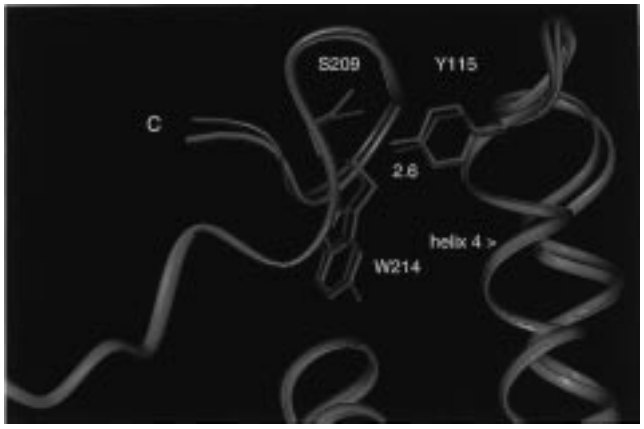

FIGURE 6: Superposition of residues near the end of helix 4 and the C-terminal tail in subunit B. The traces of the native and (5-FTrp)$_4$ enzymes are shown in purple and green, respectively. In the native structure the hydroxyl groups of Tyr115 and Ser209 are close enough and have good geometry for formation of a hydrogen bond. Note that the hydroxyl group of Ser209 is turned away from Tyr115 in the (5-FTrp)$_4$ enzyme.

Table 5: Comparison of Selected Interatomic Distances for the Mutant and Native Proteins[a]

		interatomic distance (Å)	
atom 1	atom 2	5-FTrp	native
Y6OH (A)	GSHSG (A)	3.2	3.3
Y6OH (B)	GSHSG (B)	3.2	3.3
W7NE1 (A)	J218OE1 (A)	2.8	2.8
W7NE1 (B)	J218OE1 (B)	2.9	2.8
W45NE1 (A)	I218O5 (A)	**3.0**	**2.7**
W45NE1 (B)	J218O5 (B)	2.8	2.8
W214CE3 (A)	CYS114SG (A)	3.6	3.8
W214CE3 (B)	CYS114SG (B)	**3.4**	**3.7**
S209OG (A)	Y115OH (A)	2.7	2.8
S209OG (B)	Y115OH (B)	**3.1**	**2.6**
S209OG (A)	L211NH (A)	**3.3**	**3.6**
S209OG (B)	L211NH (B)	**3.1**	**3.8**

[a] Distances for the native enzyme are taken from PDB file 3GST (*28*). Distances exhibiting a significant (≥0.3 Å) change are shown in boldface type.

nearby Ser209, which, in the native enzyme, forms a hydrogen bond with the hydroxyl group of Tyr115. It has been previously suggested that this interaction limits product release by tying together the α4 helix and the C-terminal tail that constitute the active-site access channel (*20*). Any perturbation of this interaction might be expected to increase the mobility of the connected structural elements, α4 and the C-terminal tail, and enhance the rate of product release. This appears to be the case as the side chain of Ser209, particularly in subunit B, is turned slightly away from Tyr115 and may instead form a hydrogen bond with the backbone amide of Leu211 (Figure 6 and Table 5). Additionally, the CE3 atom of 5-FTrp214 is significantly closer to the SG of Cys114 in helix 4 (Table 5) than it is in the native structure, an interaction that may contribute to further destabilization of the α4 helix and the Tyr115−Ser209 interaction.

Although more distant from the product binding site, 5-FTrp146 may exert some influence over the rate of product release as well. This residue is located in the loop connecting the α5 and α6 helices (Figure 7). The side chain is buried such that the fluorine atom comes in close contact with the side chains of Phe183 (CE1) and Phe187 (CA, CB, and CD1). A local distortion of the chain here, due to the larger

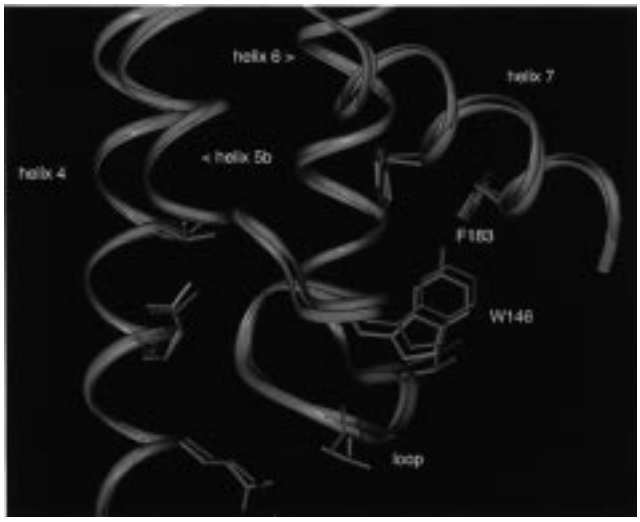

FIGURE 7: Superposition of the loop harboring Trp146. The traces of the native and (5-FTrp)$_4$ enzymes are shown in purple and green, respectively. Note the close interaction between the fluorine atom of 5-FTrp146 in the loop and the side chain of Phe183 in helix 7.

size of the fluorine atom, causes the loop region to "bump" against the C-terminal end of the α4 helix, at the N-terminus of which Tyr115 resides. This remotely transmitted interaction may also have the effect of increasing the dynamic or static disorder of portions of the α4 helix.

DISCUSSION

Binding of GSH. The preequilibrium binding of GSH to the enzyme deserves some comment with respect to both the basic characteristics of the kinetics and the lack of influence of the 5-FTrp mutations on the binding event. Most notable is the fact that the second-order rate constant for binding is significantly less than the diffusion limit for both the native enzyme and the (5-FTrp)$_4$ enzyme. The observed binding reaction, which involves the ionization of the sulfhydryl group, is a two-step process. Since GSH (not GS^-) is the major species in solution at pH 7, one reasonable scenario involves the binding of GSH followed by rapid ionization of the sulfhydryl group as illustrated:

$$E \overset{GSH}{\rightleftharpoons} E{\cdot}GSH \overset{H_2O}{\rightleftharpoons} E{\cdot}GS^- + H_3O^+ \qquad (1)$$

The proton transfer reaction is likely to be very fast and its rate can be derived from the relative pK_a values of the species. Thus, the rate constant (k_f) for proton transfer from E·GSH to water can be estimated from eq 2, given a pK_a = 6.2−6.5 for E·GSH (*14*), a pK_a = −1.74 for H_3O^+ (*32*), and assuming the rate constant for the back proton transfer is diffusion-controlled, $k_r = 10^{11}$ M^{-1} s^{-1} (*32*):

$$k_f = k_r \frac{K_a(E{\cdot}GSH)}{K_a(H_3O^+)} \approx 10^3\ M^{-1}\ s^{-1} \qquad (2)$$

Even assuming an effective water concentration at the active site that is significantly less than 55 M, the net rate of the forward proton transfer is likely to be >1000 s^{-1} and too fast to measure in the stopped-flow instrument.

One possible explanation for binding of the peptide at less than the diffusion limit is that only the minor species, GS^-, is recognized by the enzyme. In fact, if the observed rate

constants are evaluated in terms of the concentration of GS^-, then a second-order rate constant of 10^8 M^{-1} s^{-1} is obtained. However, this explanation seems unlikely for several reasons. First, there are numerous hydrogen-bonding and electrostatic interactions involved in the binding of the peptide (*14*). It seems unlikely that one would be so dominant as to control the kinetics of binding. Second, un-ionized analogues of GSH such as the oxygen analogue, GOH, bind reasonably well to the enzyme (*33*). Finally, the preionized, tight-binding analogue GSO_3^- binds with essentially the same second-order rate constant as does GSH to the $(5\text{-FTrp})_4$ enzyme (Table 3). The primary difference between the binding characteristics of GSH and GSO_3^- is in k_{off}, which is at least 20-fold smaller for GSO_3^-. This observation suggests that the off rate is significantly influenced by the protonation state of the sulfur but that the on rate is controlled by other factors.

The most likely explanation for the binding of GSH and GSO_3^- at less than the diffusion limit is that a rapid equilibrium conformational change in the enzyme is necessary before binding of the peptide, as illustrated in eq 3. Note

$$E \underset{k_{-1}}{\overset{k_1}{\rightleftharpoons}} E' \underset{k_{off}}{\overset{k_{on}[GSH]}{\rightleftharpoons}} E'\cdot GS^- \qquad (3)$$

$$k_{obs} = k_{off} + k_{on}\frac{k_1}{k_1 + k_{-1}}[GSH] \qquad (4)$$

that from the expression for k_{obs} in eq 4 that if $k_{-1} > k_1$, then the measured $k'_{on} = k_{on}[k_1/(k_1 + k_{-1})]$ is less than the actual diffusion-controlled k_{on} for the receptive conformation, E′, by a factor of $k_1/(k_1 + k_{-1})$. This situation is a commonly encountered one in the binding of ligands to macromolecules (*34*).

The indole NH of 5-FTrp should be a better hydrogen-bond donor than Trp since it has a lower pK_a. The original anticipation that the 5-FTrp substitution would tighten the binding of GSH by strengthening the two hydrogen-bonding interactions and decreasing the off rate of the peptide is clearly not the case. That there is no discernible difference in the binding kinetics is probably a manifestation of the fact that there are 13 hydrogen-bonding or electrostatic interactions that anchor GSH to the protein. Any increase in the strength of the interactions involving the indole NH is either too small to be observed or offset by subtle changes in the structure as described below.

The Fluorine Atom as a Hydrogen-Bond Acceptor. The C−F bond dipole is opposite that of a C−H bond so that fluorine-for-hydrogen substitutions alter the electrostatics near site of substitution. The fluorine atom may act as a hydrogen-bond acceptor in protein structures that involve either solvent molecules or protein donors, as was recently demonstrated in the structure of the tetradeca(3-fluorotyrosyl)glutathione transferase (*17*). In marked contrast, there are virtually no potential hydrogen-bonding interactions with the fluorine atoms observed in the structure of tetra(5-fluorotryptophanyl)glutathione transferase. The only possible exception is the 3.5 Å contact between the fluorine of 5-FTrp45 and the hydroxyl group of Tyr32 in subunit B. The paucity of possible hydrogen-bonding partners is probably a manifestation of the fact that fluorine atoms associated with the tryptophan residues are located in more inaccessible regions of the protein.

Steric Influence of Fluorine-for-Hydrogen Substitution. It is often casually stated that fluorine is an isosteric substitution for hydrogen. The tryptophan side chain is an excellent venue for testing this supposition since the indole ring is usually found buried in the interior of protein structures and closely packed with other residues. Although it is true that the van der Waals radius of fluorine is just 0.15 Å larger than that of hydrogen, the increase in size is enough to cause structural adjustments in protein architecture. Moreover, the electrostatic character of the fluorine may also contribute to repulsive interactions. Consider, for example, the interaction between the fluorine atom of 5-FTrp7 and the carbonyl oxygen of Ala33 (Figure 5B). In addition to the unfavorable van der Waals interaction there is an electrostatic repulsion between the partial negative charges on the oxygen and fluorine atoms. The structural change in domain I near the GSH binding site does not alter the interactions between GSH and the protein but, rather, is absorbed by adjustments of the main chain near 5-FTrp7.

The structural and functional adjustments associated with domain II are more apparent primarily because the side chains of 5-FTrp146 and 5-FTrp214 are in tightly packed regions of the protein where the structural changes can be transmitted to nearby regions. Although the changes are small, they may affect the dynamics of the associated structural elements as evinced by an increase in the relative *B*-factors of residues, particularly those associated with the C-terminal end of helix 4, and in the enhanced rate of product release in the reaction with CDNB. The functional properties of the $(5\text{-FTrp})_4$ enzyme are reminiscent of those of the Y115F mutant. In this instance, the enhanced catalytic activity toward CDNB (also associated with product release) was proposed to be due to the loss of the hydrogen bond between the hydroxyl group of Tyr115 and Ser209 (*20*).[4] This interaction appears to be disrupted indirectly by one or more of the 5-FTrp residues leading to similar catalytic properties.

Conclusions. Fluorinated amino acids are among the few unnatural amino acids that can be incorporated into proteins by the normal biosynthetic apparatus of the cell. The present study demonstrates that 5-fluorotryptophan can be successfully incorporated at near-quantitative levels by using a simple protein expression system. Despite the modest size difference between fluorine and hydrogen, the steric effect of the substitution is easily observed in both the three-dimensional structure and the functional properties of proteins. In the case of the rat M1-1 glutathione transferase, which has four Trp residues, including two in the active site, 5-fluorotryptophan incorporation causes a modest increase in the catalytic activity of the enzyme that is associated with the product release step. Analysis of the crystal structure of the mutant indicates that the enhanced activity cannot be directly attributed to any single fluorine atom. Rather it appears that several subtle changes together may give rise to the altered catalytic character. The structure of this

[4] The fully refined crystal structure of the Y115F mutant exhibits well above average *B*-factors for helix 4 and poor electron density for F115 (G. Xiao, R. N. Armstrong, and G. L. Gilliland, unpublished results).

enzyme, along with the structure of tetradeca(3-fluorotyrosyl)glutathione transferase, show that fluorine-for-hydrogen substitutions in macromolecular structures are not entirely benign and can result in easily measurable effects in both structure and function.

ACKNOWLEDGMENT

We thank Bryan Bernat for his assistance in making the stopped-flow kinetic measurements and Dr. Kris Tesh for help in the X-ray data collection.

REFERENCES

1. Hull. W. E., and Sykes, B. D. (1974) *Biochemistry 13*, 3431−3437.
2. Sykes, B. D., Weingarten, H. L., and Schlesinger, M. J. (1974) *Proc. Natl. Acad. Sci. U.S.A. 71*, 469−473.
3. Lu, P., Jarema, M., Mosser, K., and Daniel, W. E., Jr. (1976) *Proc. Natl. Acad. Sci. U.S.A. 78*, 3471−3475.
4. Kimber, B. J., Griffiths, D. V., Birdsall, B., King, R. W., Scudder, P., Freeney, J., Roberts, G. C. K., and Burgen, A. S. V. (1977) *Biochemistry 16*, 3492−3500.
5. Rule, G. S., Pratt, E. A., Simplaceanu, V., and Ho, C. (1987) *Biochemistry 26*, 549−556.
6. Peersen, O. B., Pratt, E. A., Truong, H.-T. N., Ho, C., and Rule, G. S. (1990) *Biochemistry 29*, 3256−3262.
7. Lui, S. M., and Cowan, J. A. (1994) *J. Am. Chem. Soc. 116*, 4483−4484.
8. Hoeltzli, S. D., and Frieden, C. (1996) *Biochemistry 35*, 16843−168451.
9. Duewel, H., Daub, E., Robison, V., and Honek, J. F. (1997) *Biochemistry 36*, 3404−3416.
10. Hoeltzli, S. D., and Frieden, C. (1998) *Biochemistry 36*, 387−398.
11. Hendrickson, W. A., Horton, J. R., and LeMaster, D. M. (1990) *EMBO J. 9*, 1665−1672.
12. Yagil, G. (1967) *Tetrahedron 23*, 2855−2861.
13. Armstrong, R. N. (1997) *Chem. Res. Toxicol. 10*, 2−18.
14. Ji, X., Zhang, P., Armstrong, R. N., and Gilliland, G. L. (1992) *Biochemistry 31*, 10169−10184.
15. Liu, S., Zhang, P., Ji, X., Johnson, W. W., Gilliland, G. L., and Armstrong, R. N. (1992) *J. Biol. Chem. 267*, 4296−4299.
16. Parsons, J. F., and Armstrong, R. N. (1996) *J. Am. Chem. Soc. 118*, 2295−2296.
17. Xiao, G., Parsons, J. F., Armstrong, R. N., and Gilliland, G. L. (1997) *J. Am. Chem. Soc. 119*, 9325−9326.
18. Leatherbarrow, R. J. (1992) *Grafit Version 3.0*, Erithacus Software Ltd., Staines, U.K.
19. Cleland, W. W. (1979) *Methods Enzymol. 63*, 103−138.
20. Johnson, W. W., Liu, S., Ji, X., Gilliland, G. L., and Armstrong, R. N. (1993) *J. Biol. Chem. 268*, 11508−11511.
21. Otwinowski, Z., and Minor, W. (1996) *Methods Enzymol. 276*, 307−326.
22. Brunger, A. T., (1992) *X-PLOR version 3.1—A system for X-ray crystallography and NMR*, Yale University Press, New Haven, CT.
23. Tronrud, D. E. (1994) *The TNT Refinement Package*, Oregon State Board of Higher Education, Eugene, OR.
24. Jones, T. A., Zou, J. Y., Cowan, S. W., and Kjeldgaard, M. (1991) *Acta Crystallogr. A47*, 110−119.
25. Laskowski, R. A., MacAurther, M. W., Moss, D. S., and Thornton, J. M., (1993) *J. Appl. Crystallogr. 26*, 283−291.
26. Jakobson, I., Warholm, M., and Mannervik, B. (1979) *J. Biol. Chem. 254*, 7085−7089.
27. Graminski, G. F., Kubo, Y., and Armstrong, R. N. (1989) *Biochemistry 28*, 3562−3568.
28. Ji, X., Johnson, W. W., Sesay, M. A., Dickert, L., Prasad, S. M., Ammon, H. L., Armstrong, R. N., and Gilliland, G. L. (1994) *Biochemistry 33*, 1043−1052.
29. Shan, S., and Armstrong, R. N. (1994) *J. Biol. Chem. 269*, 32373−32379.
30. Liu, S., Ji, X., Gilliland, G. L., Stevens, W. J., and Armstrong, R. N. (1993) *J. Am. Chem. Soc. 115*, 7910−7911.
31. Xiao, G., Liu, S., Ji, X., Johnson, W. W., Chen, J., Parsons, J. F., Stevens, W. J., Gilliland, G. L., and Armstrong, R. N. (1996) *Biochemistry 35*, 4753−4765.
32. Bender, M. L. (1971) *Mechanisms of Homogeneous Catalysis from Protons to Proteins*, p 23, John Wiley, New York.
33. Chen, W.-J., Boehlert, C. C., Rider, K., and Armstrong, R. N. (1985) *Biochem. Biophys. Res. Commun. 128*, 233−240.
34. Johnson, K. A. (1992) *Enzymes 20*, 1−61.

BI980219E